

Shot-to-shot and average absolute photon flux measurements of a femtosecond laser high-order harmonic photon source

This content has been downloaded from IOPscience. Please scroll down to see the full text.

2011 New J. Phys. 13 093003

(<http://iopscience.iop.org/1367-2630/13/9/093003>)

View [the table of contents for this issue](#), or go to the [journal homepage](#) for more

Download details:

IP Address: 131.169.95.214

This content was downloaded on 08/09/2016 at 10:31

Please note that [terms and conditions apply](#).

You may also be interested in:

[Pulse energy measurements of EUV undulator radiation](#)

Alexander Gottwald, Ralph Müller, Mathias Richter et al.

[Cut-off scaling of high-harmonic generation driven by a femtosecond visible optical parametric amplifier](#)

Giovanni Cirimi, Chien-Jen Lai, Eduardo Granados et al.

[Metrology of high-order harmonics for free-electron laser seeding](#)

C Erny, E Mansten, M Gisselbrecht et al.

[Ultraviolet and vacuum-ultraviolet detector-based radiometry at the Metrology Light Source](#)

Alexander Gottwald, Udo Kroth, Mathias Richter et al.

[Spectral characterization of fully phase-matched high harmonics generated in a hollow waveguide for free-electron laser seeding](#)

F Ardana-Lamas, G Lambert, A Trisorio et al.

[Boosting laboratory photoelectron spectroscopy by megahertz high-order harmonics](#)

Cheng-Tien Chiang, Michael Huth, Andreas Trützschler et al.

Shot-to-shot and average absolute photon flux measurements of a femtosecond laser high-order harmonic photon source

T Leitner^{1,6}, A A Sorokin^{2,3,5}, J Gaudin⁴, H Kaser², U Kroth²,
K Tiedtke³, M Richter² and Ph Wernet¹

¹ Institut für Methoden und Instrumentierung der Forschung mit
Synchrotronstrahlung, Helmholtz-Zentrum Berlin für Materialien und Energie
GmbH, Albert-Einstein-Str. 15, 12489 Berlin, Germany

² Physikalisch-Technische Bundesanstalt, Abbestr. 2-12, 10587 Berlin,
Germany

³ Deutsches Elektronen-Synchrotron DESY, Notkestr. 85, 22607 Hamburg,
Germany

⁴ European XFEL, Albert-Einstein-Ring 19, 22761 Hamburg, Germany

⁵ Ioffe Physico-Technical Institute, Polytekhnicheskaya 26,
194021 St Petersburg, Russia

E-mail: leitner@helmholtz-berlin.de

New Journal of Physics **13** (2011) 093003 (11pp)

Received 5 January 2011

Published 1 September 2011

Online at <http://www.njp.org/>

doi:10.1088/1367-2630/13/9/093003

Abstract. The absolute flux of a femtosecond vacuum-ultraviolet (VUV) photon source based on the high-order harmonic generation of a femtosecond Ti:sapphire laser and monochromatized with a grating monochromator is determined both on a shot-to-shot basis and averaged over seconds by a calibrated gas monitor detector. The average flux is compared with the average flux as determined with a calibrated GaAsP semiconductor photodiode. We found that the photodiode is a reliable and easy-to-use tool for estimating the order of magnitude of the average photon flux but that, due to saturation losses, it underestimates the average flux by up to -15% .

⁶ Author to whom any correspondence should be addressed.

Contents

| | |
|---|----------|
| 1. Introduction | 2 |
| 2. Experimental setup | 3 |
| 3. Purity and single ionization of the target gas | 5 |
| 4. Shot-to-shot distribution | 5 |
| 5. Comparison of the diode versus the gas monitor detector | 6 |
| 6. Summary | 9 |
| References | 9 |

1. Introduction

High-order harmonic generation (HHG) has emerged as a widely used tool for producing bright femto- and attosecond vacuum-ultraviolet (VUV) and soft x-ray pulses [1–4]. These pulses can be used to study ultrafast atomic, molecular and magnetism dynamics [5–9] and are bright enough for performing coherent x-ray diffractive imaging for investigations on the nanoscale [10]. Furthermore, the HHG process itself can provide insights into the electronic structure of the generating molecule [11–16].

One of the key parameters of every photon source is its photon flux. Determination of the absolute flux and of the shot-to-shot fluctuations of the flux is highly desirable. Correct determination of these parameters becomes particularly important when exploring the feasibility of new experiments. For example, the photon flux is a crucial parameter when high-harmonic radiation is used to seed a free electron laser (FEL) [17, 18]. Accurate on-line measurements of the photon flux are required when HHG sources are used to investigate nonlinear effects in the VUV-spectral range, e.g. for the determination of atomic two-photon ionization cross sections [19, 20]. In general, the absolute flux and the shot-to-shot fluctuations are key parameters when optimizing an existing or setting up a new HHG source.

To our knowledge, accurate shot-to-shot measurements of absolute fluxes from HHG sources have not been made yet. Nisoli *et al* [21] measured shot-to-shot HHG spectra, but did not determine shot-to-shot fluxes. Determination of absolute average fluxes of an HHG source was performed in [22] based on a rather complicated scintillator-photomultiplier setup. In [23], a calibrated extreme UV spectrometer was used to determine absolute photon fluxes but with a standard uncertainty as high as 50%.

Other widely used, easy-to-use tools for measuring photon fluxes are semiconductor photodiodes. In [17, 24, 25] for example, they are used to determine absolute average photon fluxes of HHG sources. Such photodiodes are usually calibrated at quasi-continuous-wave (cw) light sources with long pulses in the picosecond regime at high repetition rates (e.g. synchrotrons). The Physikalisch-Technische Bundesanstalt (PTB; Germany's national metrology institute) uses the Metrology Light Source for the calibration of photodiodes in the UV-VUV regime [26]. At the normal-incidence monochromator beamline for UV and VUV detector calibration, pulses of 20 ps pulse duration (full-width at half-maximum (FWHM)) are delivered with a repetition rate of 500 MHz and peak fluxes of $5 \times 10^{11} \text{ photons s}^{-1}$ (i.e. $10 \text{ photons pulse}^{-1}$). In contrast to that, our HHG setup delivers monochromatized 120 fs FWHM pulses at a repetition rate of 3 kHz with peak fluxes of the order of $10^{19} \text{ photons s}^{-1}$ (i.e. $10^6 \text{ photons pulse}^{-1}$). The average radiant power and the spot size of the diode for these

two sources are comparable, hence the average photon flux density is too. Thus, if the HHG photon flux is measured with a photodiode, the peak flux or the peak radiant power, respectively, seen by this diode are more than seven orders of magnitude higher than during calibration. This raises the question of whether the calibration is still correct or whether saturation losses significantly contribute to the diode's response in the regime of parameters used here. The rapid generation of a large number of charge carriers in the active area of the diode from femtosecond pulses will not necessarily result in the same response as illuminating the diode with a (quasi)-cw light source of comparable average power. Enhanced recombination may occur, leading to increased saturation loss, meaning that fewer generated charge carriers reach the read-out electronics and contribute to the diode's response signal. This effect should intensify with increasing charge carrier density generated by increasing peak powers of the radiation. Therefore saturation loss and erroneous response of the photodiode will rise as well [27–29]. In order to test whether semiconductor photodiodes are reliable for measuring the absolute photon fluxes of high-peak-power femtosecond sources, we compared the values for the average photon flux of the monochromatized radiation available for experiments from our source measured with a calibrated GaAsP semiconductor photodiode (Hamamatsu model g112704) with those obtained from measurements with a calibrated and validated gas monitor detector (GMD). The GMD is based on the photoionization of a (rare) gas and was developed by PTB/DESY/Ioffe Institute for the on-line measurement of the radiant power of VUV and soft x-ray FELs [30–33]. Measurement of absolute average photon fluxes as well as shot-to-shot fluctuations with an accuracy of 5% is feasible with this device.

2. Experimental setup

Our experimental setup is shown in figure 1; see also [34, 35]. The VUV radiation is produced by a 50 fs, 1 mJ Ti:sapphire laser (central wavelength 785 nm), which is focused into a 5.5 mm long gas cell by an $f = 500$ mm lens, resulting in a focal spotsize of $60\text{ }\mu\text{m}$ and a peak intensity of approximately $2 \times 10^{14}\text{ W cm}^{-2}$. The entrance and exit of the cell along the laser path are sealed with a thin copper foil (0.1 mm) in which the laser itself drills optimum-sized holes for propagating through. In this experiment, we use either Xe or Ar as a nonlinear medium for generation. We operate the cell at a pressure in the gas inlet tube of 0.46 mbar for Xe and 3.2 mbar for Ar and a background pressure outside the cell of 8×10^{-3} or 1.1×10^{-2} mbar, respectively. Thereafter the infrared (IR) light is blocked by two aluminum foils (150 nm thick) one before and one after a toroidal grating monochromator to ensure that no fundamental IR photons reach the GMD or the photodiode and influence the measurements, although both detectors are not sensitive to the IR radiation. The monochromatized VUV pulses then first pass the GMD before they hit the photodiode. The pulse duration available for experiments after the monochromator is ~ 120 fs FWHM in our setup. This was determined by VUV-IR cross correlation with photoionization sidebands of Ar, as demonstrated in [36]. The cross correlation measurement was made in a separate experiment to ensure that no other gas from the photoionization chamber perturbs the GMD signal. The bandwidth of the monochromatized pulses amounts to ~ 140 meV, as shown in an earlier work [34]. We performed the experiment with four different harmonics of the IR laser (H11, H13, H15 and H17) at corresponding photon energies of 17.4, 20.5, 23.7 and 26.9 eV. The GMD is based on atomic photoionization of a rare gas at low particle density in the range of 10^{11} – 10^{12} cm^{-3} . Therefore, it is indestructible and transmits more than 99.5% of the radiation for the photon energy range used in this

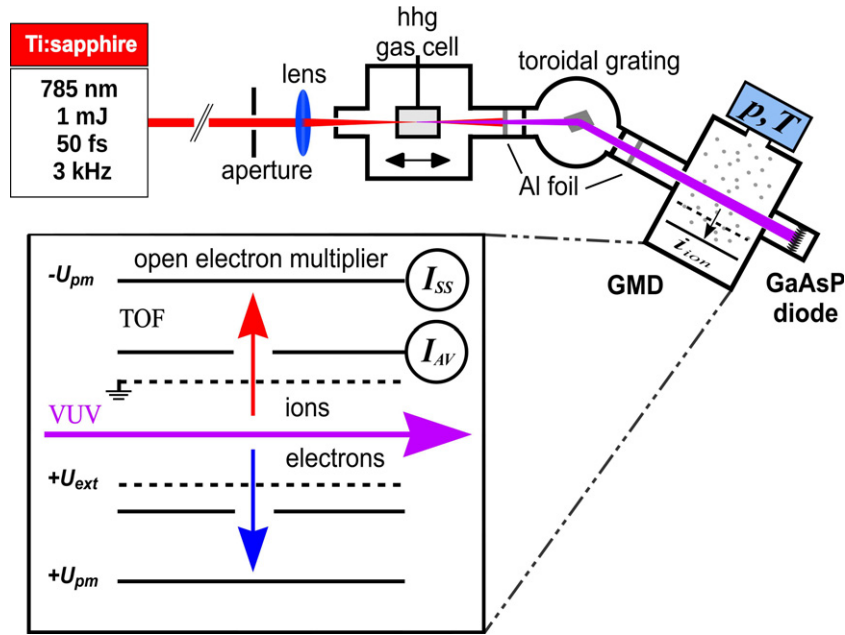


Figure 1. Experimental setup—a 50 fs Ti:sapphire laser drives the HHG VUV source; after a toroidal grating, the photon flux in the monochromatized VUV beam is measured by the GMD and a standard Hamamatsu GaAsP photodiode. Inset: (principal) sketch of the assembly inside the GMD, illustrating its basic functional principle; I_{SS} and I_{AV} denote the single-shot and average signals available from the detector.

experiment [37]. The inset of figure 1 illustrates the functional principle of this detector. The VUV radiation ionizes the target gas (either Xe or Ar in this work). The generated ions and electrons are extracted and accelerated in opposite directions by a homogeneous static electric field. The extraction field of 333 V cm^{-1} (corresponding to an extraction voltage of 1000 V) is chosen to be high enough to ensure complete collection of the charged particles created in the interaction volume accepted by the respective particle detector. In the present experiment, only the ion signal was measured. A first simple metal plate detection electrode allows us to measure a slow averaging current I_{AV} using a calibrated Keithley 617 electrometer with a time constant of a few seconds, which is not affected by any individual intra-pulse time structure or shot-to-shot variations of the radiation. Moreover, a fraction of the ions enter a drift section through a small aperture in the detection electrode and are detected by an open electron multiplier (ETP 14880) operated in a linear regime. The multiplier can be used for ion time-of-flight (TOF) spectrum measurements, which enables us to check the purity of the target gas as well as the possible influence of multi-photon ionization on our measurements, as will be discussed later. Furthermore, it can be utilized for pulse-resolved (shot-to-shot) relative flux measurements. The signal from the multiplier is read out with the help of a LeCroy digital oscilloscope.

From the measured ion-current signal I_{ion} , the average number of photons N_{ph} can be calculated as

$$N_{ph} = k_{cal} \times \frac{I_{ion}}{n_a(p, T) \times \sigma_{pi}(h\nu)}, \quad (1)$$

where σ_{pi} is the photoionization cross section of the target gas at the used photon energy $h\nu$ and k_{cal} is a known detector calibration constant including the length along the photon beam accepted by the detection electrode and the ion detection efficiency. n_a is the target gas density at a given pressure and temperature, determined by $n_a = p/k_B T$ (k_B the Boltzmann constant). As knowing the exact pressure p and temperature T of the target gas is crucial for deriving the correct photon flux from the ion-current signal, a calibrated spinning rotor vacuum gauge for monitoring gas pressures in the range of 10^{-4} mbar and a calibrated Pt100 resistance thermometer are installed in the device. In equation (1), the target gas density n_a is derived from the pressure p and temperature T (p and T usually remain constant during one experimental session); the photoionization cross section σ_{pi} was tabulated in [31]. The GMD was calibrated in ion-current mode at the PTB Laboratories in the VUV spectral range using dispersed synchrotron radiation at low intensity in conjunction with a cryogenic radiometer, which is a primary detector standard [26]. The relative standard uncertainty of the calibration factor amounts to 3.4%. Taking into account the uncertainty of the ion-current measurement of 1.5%, the pressure measurement of 1.4%, the temperature measurement of 1.0% and the uncertainty of the cross section data of 3%, the final relative standard uncertainty for the average photon flux determination with the GMD amounts to 5%. This value is also justified by validation measurements made at the Spring-8 FEL facility in Japan [32, 33] recently.

3. Purity and single ionization of the target gas

We checked the TOF spectra available from the multiplier signal of the GMD to rule out the influence of contaminating impurities in the target gas and the influence of multiple ionization of the target gas. Both effects would perturb the ion-current signal by adding currents from other ions than singly ionized target gas particles and therefore the absolute calibration would no longer be valid. Figure 2(a) shows an ion TOF spectrum where the Xe target gas was contaminated with traces of residual air. Besides the Xe ion peak, N_2 and O_2 ion peaks are clearly discernible. The TOF spectrum in figure 2(b) was taken with pure Xe as the target gas and accordingly only one peak from singly ionized Xe is discernible. Multiply ionized Xe would show up as peaks at shorter TOFs ($\text{TOF} \propto (q/m)^{-2}$) and indicate that either the peak irradiance and/or the target gas density inside the detection chamber is too high. Apparently these peaks are not present. The same purity check was performed when Ar was used as the target gas in the GMD. This purity of the spectra proves that the values of the photon numbers calculated from the GMD in our experiment are reliable.

4. Shot-to-shot distribution

Another feature of the detector is the possibility of deriving single-shot intensities from the multiplier signal. Knowing the averaged photon number N_{AV} , single-shot photon numbers, determined from the peak value of the multiplier signal I_{SS} , read as

$$N_{\text{SS}} = N_{\text{AV}} \times \frac{I_{\text{SS}}}{I_{\text{AV}}}. \quad (2)$$

Figure 3 shows the shot-to-shot flux variation from our laser system measured with a standard IR photodiode (leakage through a mirror) and the corresponding flux variation of our HHG

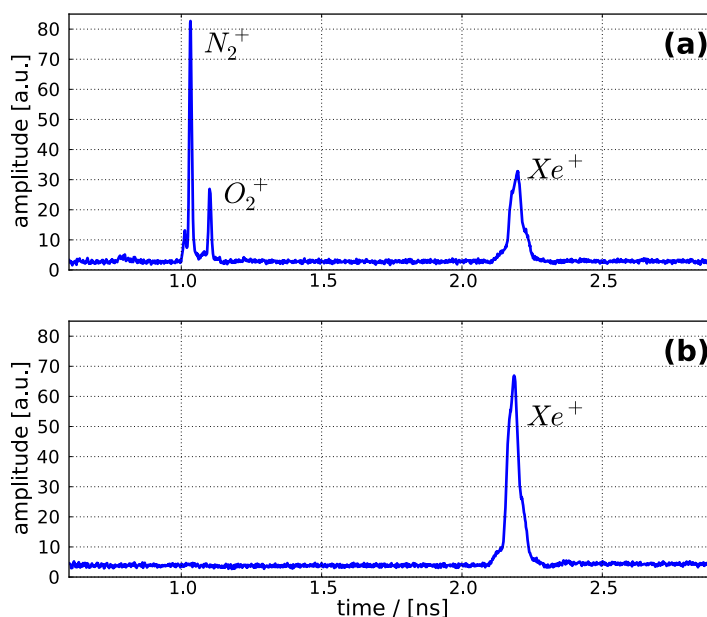


Figure 2. Two exemplary ion TOF spectra (averaged over ~ 5000 shots) from the GMD, illustrating the purity of the target gas. The spectrum of Xe target gas and residual air is shown in panel (a), while panel (b) shows the spectrum of Xe target gas as used for the flux measurements.

source measured with the single-shot multiplier signal I_{SS} coupled to a digital oscilloscope. The laser varied by $\pm 2.3\%$ at FWHM, whereas the HHG signal varied by $\pm 26.6\%$. The fact that the VUV signal fluctuates by an order of magnitude more than the generating laser clearly points out the highly nonlinear nature of the HHG process. Note that the source was not optimized for minimal shot-to-shot fluctuations.

5. Comparison of the diode versus the gas monitor detector

Figures 4 and 5 depict a comparison of the average flux measured with the GMD and the GaAsP photodiode. The diode was calibrated in the range 6–27 eV by PTB within one week of the experiments at the HHG source to foreclose errors due to a diode-specific history such as, for example, aging processes. The source used for calibration delivered approximately $10 \text{ photons pulse}^{-1}$ with a pulse duration of 20 ps FWHM and a bandwidth of 0.4 eV at a repetition rate of 500 MHz. This corresponds to an average flux of $5 \times 10^9 \text{ photons s}^{-1}$ or an average power of 20 nW at 23.7 eV. The peak flux of a single pulse is thus of the order of $5 \times 10^{11} \text{ photons s}^{-1}$ corresponding to a peak power of $2 \mu\text{W}$. In contrast, our HHG setup yields monochromatized pulses with $10^6 \text{ photons pulse}^{-1}$ of 120 fs FWHM duration and a bandwidth of 140 meV at a repetition rate of 3 kHz. This corresponds to an average flux of $3 \times 10^9 \text{ photons s}^{-1}$ or an average power of 12 nW. Due to the short duration of the pulses, the peak flux of a single pulse is of the order of $10^{19} \text{ photons s}^{-1}$, which corresponds to a peak power of 45 W for a photon energy of 23.7 eV as used here. We want to point out that for both cases, the irradiated area of the diode was 2–3 mm². For comparing both detectors, we calculated the

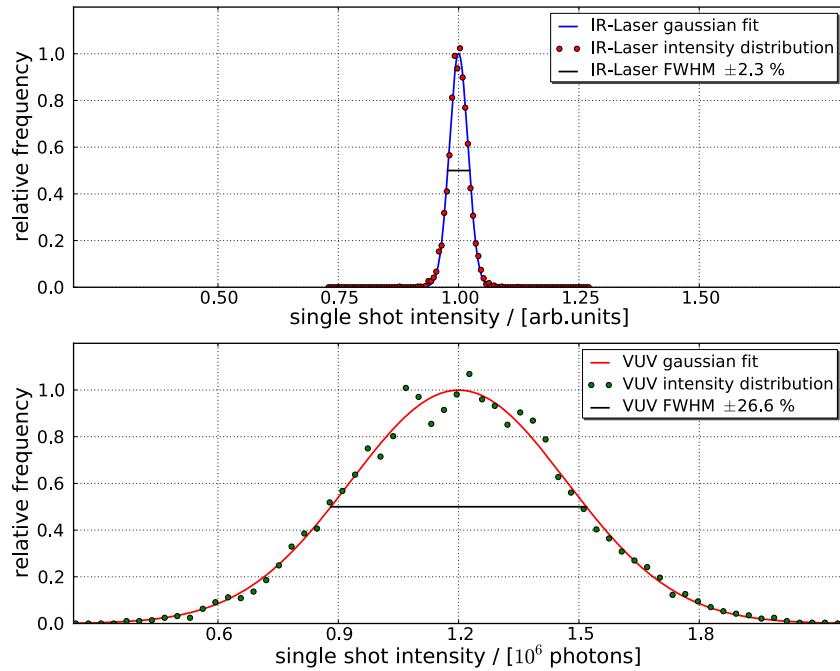


Figure 3. Intensity distribution, showing the relative shot-to-shot energy variations of the fundamental IR laser (top) and the VUV radiation produced in the highly nonlinear HHG process (bottom). The IR laser intensity distribution in the upper panel is normalized to its maximum and shown in arbitrary units, whereas absolute photon numbers are given for the VUV intensity distribution.

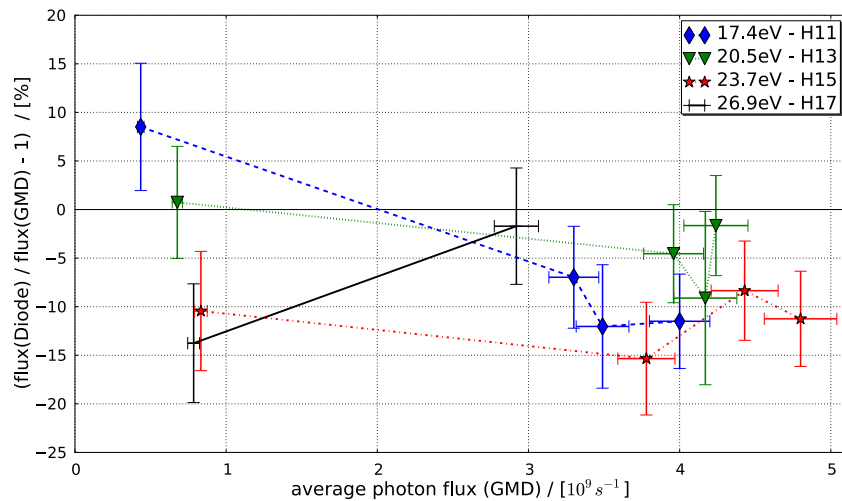


Figure 4. Plot of the relative deviation of the average photon flux determined with the photodiode from the absolute flux given by the calibrated gas detector signal versus the photon flux for different photon energies. The measurements with different laser harmonics are connected with lines and correspond to various flux levels. \blacklozenge , H11, $+$, H13, \star , H15, \blacktriangledown , H17.

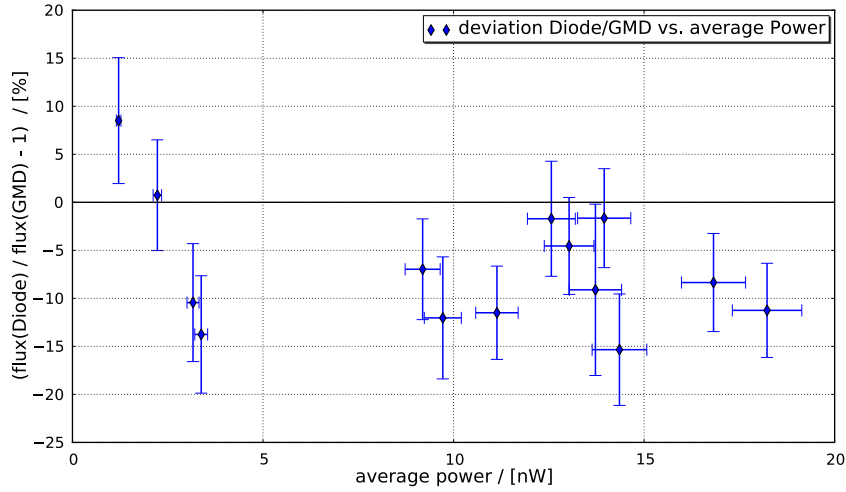


Figure 5. Plot of the relative deviation of the average photon flux measured with the photodiode from the absolute flux given by the calibrated GMD signal versus the average power deposited in the diode for the measurements from figure 4. The diode systematically underestimates the photon flux by up to -15% for all but the two smallest amounts of power tested in this experiment.

relative deviation between the fluxes determined from the diode and GMD:

$$\Delta = \frac{\text{flux(Diode)}}{\text{flux(GMD)}} - 1. \quad (3)$$

In figure 4, the relative deviation (in percentage) between the average photon flux derived from the diode signal and that from the GMD is plotted against the absolute average flux measured with the GMD. Four data sets (connected with lines) are shown for four different photon energies corresponding to different harmonics of our source. To vary the harmonic yield and therefore the fluxes, the width of an aperture in the generating laser beam was tuned. In the next step, we calculated the resulting power (the product of photon energy and flux) of the VUV radiation. In figure 5, the deviation (in percentage) between the average photon flux calculated from the response of the diode and that calculated from the GMD is plotted against the absolute average power given by the GMD signal. The error bars in both graphs are deduced by taking into account the 5% accuracy of the GMD and the accuracy in the measurement of the photo current from the diode. The photo current was measured with a Keithley 6485 electrometer in slow averaging mode. The accuracy of the photo current values was approximated for every measurement by carefully observing the variation of the photo current signal, and was in the range of 3–10%. The graphs show that the diode systematically underrated the photon flux by up to -15% . This points to saturation effects in the diode due to the high peak power emitted from our HHG source. From work using pulsed classical laser sources [27–29], it is known that due to the increasing probability of charge carrier recombination in the diode with increasing peak power, the charge yield from the diode is lower than expected from the calibration with radiation at comparable average powers. Illuminating a diode with quasi-cw light provokes an almost constant creation of charge carriers in the semiconductor material and yields an equilibrium between charge carriers created by the radiation, recombination of charge carriers and charge arriving at the read-out electronics of the diode. When the diode is

instead illuminated with short femtosecond pulses of high peak power separated by relatively long dark periods without illumination, there is more time for the charge carriers to recombine before being read out. The rate of recombination depends directly on the charge carrier density, which in turn depends directly on the instantaneous power hitting the diode. Thus, at high peak powers, higher recombination rates and therefore saturation losses occur. This explains the saturation effects observed here: the response of the semiconductor diode for short pulses is lower than those expected from calibration with longer pulses. Typical saturation behavior such as increasing deviation for increasing fluxes could not be determined from our data due to the small dynamic range that was available in this work.

However, our results prove that a calibrated photodiode is still a good and easy-to-use tool for measuring the flux of femtosecond VUV HHG photon sources to within, as in our case, an accuracy of 15%.

6. Summary

For the first time, a GMD was used to measure the absolute photon flux and the absolute power of a femtosecond VUV HHG source with an accuracy of 5%. The GMD allows for the determination of absolute average fluxes, as well as shot-to-shot variations; therefore we were able to estimate the shot-to-shot stability of our 3 kHz repetition rate HHG source.

We compared average photon fluxes of four different photon energies and the corresponding radiant powers of our source derived from a PTB-calibrated Hamamatsu g112704 GaAsP photodiode with the values obtained from the GMD. In our experiment, the photodiode systematically underestimated the real photon flux by up to -15% . This points to saturation losses in the diode due to increased recombination of the charge carriers generated by the incident light, but also shows that such a semiconductor photodiode is still a good tool for estimating the average flux from femtosecond VUV sources with an accuracy of 15% in our case.

Photodiodes have been used to measure the photon flux in many experiments; the present work clarifies the reliability and accuracy of the photon fluxes determined in these experiments and justifies the use of semiconductor photodiodes to measure the photon flux of a femtosecond HHG source for future experiments.

References

- [1] L'Huillier A and Balcou Ph 1993 High-order harmonic generation in rare gases with a 1 ps 1053 nm laser *Phys. Rev. Lett.* **70** 774–7
- [2] Chen M-C, Arpin P, Popmintchev T, Gerrity M, Zhang B, Seaberg M, Popmintchev D, Murnane M and Bright K H 2010 Coherent, ultrafast soft x-ray harmonics spanning the water window from a tabletop light source *Phys. Rev. Lett.* **105** 173901
- [3] Brabec T and Krausz F 2000 Intense few-cycle laser fields: Frontiers of nonlinear optics *Rev. Mod. Phys.* **72** 545–91
- [4] Krausz F and Ivanov M 2009 Attosecond physics *Rev. Mod. Phys.* **81** 163–234
- [5] Wernet Ph, Odelius M, Godehusen K, Gaudin J, Schwarzkopf O and Eberhardt W 2009 Real-time evolution of the valence electronic structure in a dissociating molecule *Phys. Rev. Lett.* **103** 013001
- [6] Loh Z-H and Leone S 2008 Ultrafast strong-field dissociative ionization dynamics of CH_2Br_2 probed by femtosecond soft x-ray transient absorption spectroscopy *J. Chem. Phys.* **128** 204302

- [7] Gagnon E, Ranitovic P, Tong X-M, Cocke C, Murnane M, Kapteyn H and Sandhu A 2007 Soft x-ray-driven femtosecond molecular dynamics *Science* **317** 1374–8
- [8] Miaja-Avila L, Saathoff G, Mathias S, Yin J, La-O-Vorakiat C, Bauer M, Aeschlimann M, Murnane M and Kapteyn H 2008 Direct measurement of core-level relaxation dynamics on a surface-adsorbate system *Phys. Rev. Lett.* **101** 046101
- [9] La-O-Vorakiat C *et al* 2009 Ultrafast demagnetization dynamics at the *m* edges of magnetic elements observed using a tabletop high-harmonic soft x-ray source *Phys. Rev. Lett.* **103** 257402
- [10] Ravasio A *et al* 2009 Single-shot diffractive imaging with a table-top femtosecond soft x-ray laser-harmonics source *Phys. Rev. Lett.* **103** 028104
- [11] Wörner H, Bertrand J, Corkum P and Villeneuve D 2010 High-harmonic homodyne detection of the ultrafast dissociation of Br₂ molecules *Phys. Rev. Lett.* **105** 103002
- [12] Sukiasyan S, Patchkovskii S, Smirnova O, Brabec T and Ivanov M 2010 Exchange and polarization effect in high-order harmonic imaging of molecular structures *Phys. Rev. A* **82** 043414
- [13] Itatani J, Levesque J, Zeidler D, Niikura H, Pepin H, Kieffer J, Corkum P and Villeneuve D 2004 Tomographic imaging of molecular orbitals *Nature* **432** 867–71
- [14] Li W, Zhou X, Lock R, Patchkovskii S, Stolow A, Kapteyn H and Murnane M 2008 Time-resolved dynamics in N₂O₄ probed using high harmonic generation *Science* **322** 1207–11
- [15] Caillat J, Maquet A, Haessler S, Fabre B, Ruchon T, Salieres P, Mairesse Y and Taieb R 2011 Attosecond resolved electron release in two-color near-threshold photoionization of N₂ *Phys. Rev. Lett.* **106** 093002
- [16] Haessler S *et al* 2009 Phase-resolved attosecond near-threshold photoionization of molecular nitrogen *Phys. Rev. A* **80** 011404
- [17] He X *et al* 2009 Spatial and spectral properties of the high-order harmonic emission in argon for seeding applications *Phys. Rev. A* **79** 063829
- [18] Lambert G *et al* 2008 Injection of harmonics generated in gas in a free-electron laser providing intense and coherent extreme-ultraviolet light *Nat. Phys.* **4** 296–300
- [19] Nabekawa Y, Hasegawa H, Takahashi E J and Midorikawa K 2005 Production of doubly charged helium ions by two-photon absorption of an intense sub-10-fs soft x-ray pulse at 42 eV photon energy *Phys. Rev. Lett.* **94** 043001
- [20] Hasegawa H, Takahashi E J, Nabekawa Y, Ishikawa K L and Midorikawa K 2005 Multiphoton ionization of He by using intense high-order harmonics in the soft-x-ray region *Phys. Rev. A* **71** 023407
- [21] Nisoli M, Sansone G, Stagira S, De Silvestri S, Vozzi C, Pascolini M, Poletto L, Villoresi P and Tondello G 2003 Effects of carrier-envelope phase differences of few-optical-cycle light pulses in single-shot high-order-harmonic spectra *Phys. Rev. Lett.* **91** 213905
- [22] Riedel D, Hernandez-Pozos J, Palmer R, Baggott S, Kolasinski K and Foord J 2001 Tunable pulsed vacuum ultraviolet light source for surface science and materials spectroscopy based on high-order harmonic generation *Rev. Sci. Instrum.* **72** 1977–83
- [23] Sommerer G, Mevel E, Hollandt J, Schulze D, Nickles P V, Ulm G and Sandner W 1998 Absolute photon number measurement of high-order harmonics in the extreme uv *Opt. Commun.* **146** 347–55
- [24] Schnürer M, Cheng Z, Hentschel M, Tempea G, Kálmán P, Brabec T and Krausz F 1999 Absorption-limited generation of coherent ultrashort soft-x-ray pulses *Phys. Rev. Lett.* **83** 722–5
- [25] Hergott J-F, Kovacev M, Merdji H, Hubert C, Mairesse Y, Jean E, Breger P, Agostini P, Carré B and Salieres P 2002 Extreme-ultraviolet high-order harmonic pulses in the microjoule range *Phys. Rev. A* **66** 021801
- [26] Gottwald A, Kroth U, Richter M, Schoeppe H and Ulm G 2010 Ultraviolet and vacuum-ultraviolet detector-based radiometry at the metrology light source *Meas. Sci. Technol.* **21** 125101
- [27] Richter M, Kroth U, Gottwald A, Gerth Ch, Tiedtke K, Saito T, Tassy I and Vogler K 2002 Metrology of pulsed radiation for 157-nm lithography *Appl. Opt.* **41** 7167–72
- [28] Vest R and Grantham S 2003 Response of a silicon photodiode to pulsed radiation *Appl. Opt.* **42** 5054–63
- [29] Vest R, Hill S and Grantham S 2006 Saturation effects in solid-state photodiodes and impact on EUVL pulse energy measurements *Metrologia* **43** S84

- [30] Richter M *et al* 2003 Measurement of gigawatt radiation pulses from a vacuum and extreme ultraviolet free-electron laser *Appl. Phys. Lett.* **83** 2970–2
- [31] Tiedtke K *et al* 2008 Gas detectors for x-ray lasers *J. Appl. Phys.* **103** 094511
- [32] Saito N *et al* 2010 Radiometric comparison for measuring the absolute radiant power of a free-electron laser in the extreme ultraviolet *Metrologia* **47** 21
- [33] Kato M *et al* 2010 Measurement of the single-shot pulse energy of a free electron laser using a cryogenic radiometer *Metrologia* **47** 518
- [34] Wernet Ph, Gaudin J, Godehusen K, Schwarzkopf O and Eberhardt W 2011 Femtosecond time-resolved photoelectron spectroscopy with a vacuum-ultraviolet photon source based on laser high-order harmonic generation *Rev. Sci. Instrum.* **82** 063114
- [35] Wernet Ph, Godehusen K, Schwarzkopf O and Eberhardt W 2007 *Femtosecond VUV Photon Pulses for Time-Resolved Photoelectron Spectroscopy* ed P Corkum, D M Jonas, R J D Miller, A M Weiner, F P Schäfer, J P Toennies and W Zinth *Ultrafast Phenomena XV (Springer Series in Chemical Physics vol 88)* (Berlin: Springer) pp 45–7 doi:[10.1007/978-3-540-68781-8_15](https://doi.org/10.1007/978-3-540-68781-8_15)
- [36] Glover T E, Schoenlein R W, Chin A H and Shank C V 1996 Observation of laser assisted photoelectric effect and femtosecond high order harmonic radiation *Phys. Rev. Lett.* **76** 2468–71
- [37] Henke B, Gullikson E and Davis J 1993 X-ray interactions: photoabsorption, scattering, transmission and reflection at $E = 50\text{--}30\,000\text{ eV}$, $Z = 1\text{--}92$. *At. Data Nucl. Data Tables* **54** 181–342